Adsorption of phenylacetylene on Si(100)-2×1: Reaction mechanism and formation of a styrene-like π-conjugation system

Feng Tao,[1] Ming Hua Qiao,[2] Zhen Hua Li,[2] Lei Yang,[1] Yu Jing Dai,[1] Hai Gou Huang,[1] and Guo Qin Xu[1,*]

[1]*Department of Chemistry, National University of Singapore, 10 Kent Ridge, Singapore, 119260*
[2]*Department of Chemistry, Fudan University, Shanghai, People's Republic of China, 200433*

The interactions of phentylacetylene and phenylacetylene-α-d_1 with Si(100)-2×1 have been studied as a model system to mechanistically understand the adsorption of conjugated π-electron aromatic substitutions on Si(100)-2×1. Vibrational signatures show that phenylacetylene covalently binds to the surface through a [2+2]-like cycloaddition pathway between the external C≡C and Si═Si dimer, forming styrene-like conjugation structure which was further supported by the chemical-shift of C $1s$ core level. These experimental results are consistent with the density-functional theory [B3LYP/6-311//+G(d)] calculations. The resulting styrene-like conjugation structures may possibly be employed as an intermediate for further organic syntheses and fabrication of molecular architecture for modification and functionalization of Si surfaces, or as a monomer for polymerization on Si surfaces.

PACS number(s): 68.43.Fg, 82.65.+r

I. INTRODUCTION

Organic functionalization of semiconductor surfaces[1-9] has great potential applications in the development of sensitive Si-based nanosensors[10] and synthesis of ultrathin organic films for advanced optical, electronic, and biorelated devices.[7-10]

To successfully incorporate molecular functionalities into device fabrication, the most important step is to gain a thorough understanding for the formation mechanisms and binding structure of multifunctional organic molecules on Si surfaces and create precursor templates with desired reactive functionalities for further developing multilayered Si-based molecular systems. Most of the previous work in this area focused on the studies of attachment chemistry of some simple unsaturated hydrocarbons on Si surfaces.[2] However, in order to extend the organic modification and functionalization to allow for the next-layer growth, multifunctional molecules are preferred for initial binding. Upon covalent binding, this layer acting as a precursor, in turn, should retain or newly produce (during the interaction with Si surfaces) one or more reactive functional groups for the further binding of other organic molecules. The formation of surface intermediates containing delocalized π-electron structures is of particular interest due to the possibility of synthesizing larger oligomers and polymers known as semiconductors or metals[11,12] through their conjugated structures in vacuum.

Si(100)-2×1 is a semiconductor surface of technological importance. In its (2×1) reconstructed structure,[13] adjacent Si atoms pair into Si═Si dimers, shown in Fig. 1(a). The bonding within a surface dimer can be formally described in the terms of a σ bond coupled with a π bond, analogous to the C═C double bonds of alkenes, suggesting a possible similarity of chemical reactivities between them. Due to the large Si-Si distance and bending back bonds that connect the surface dimer with the bulk atoms, the π bond in a Si═Si dimer is quite weak. In fact, the Si═Si dimer might be regarded as a *di* radical as schematically presented in Fig. 1(b).

Previous studies showed that simple organic molecules containing C═C can be covalently bound to Si(100)-2×1 by a so-called "asymmetric [2+2] cycloaddition."[14-20] The asymmetric geometry of ground-state dimers allows the [2+2] reaction to proceed through an asymmetric pathway, where alkene approaches the titled Si═Si dimer from one side [Fig. 1(c)]. This asymmetric approach is of lower symmetry and can occur with a lower energy barrier. Conjugated dienes or multienes[21-24] can be covalently bonded to Si(100)-2×1 through [4+2]-like or/and [2+2]-like cycloaddition strategies. For six-membered aromatic molecules and their substitutions,[25-34] their binding mechanisms are
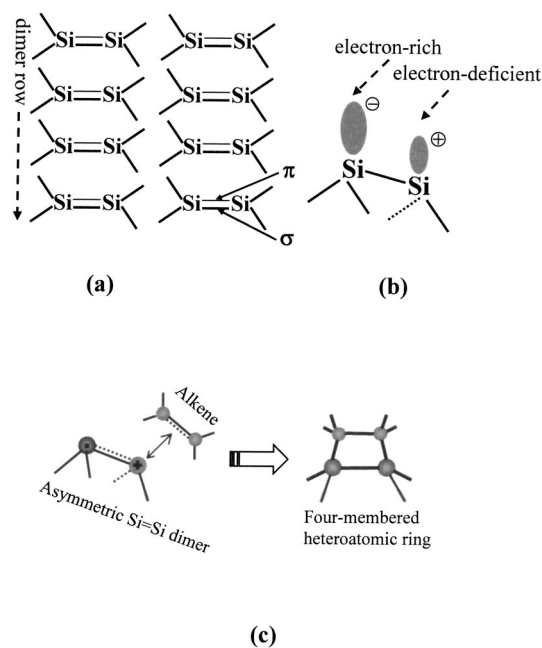

FIG. 1. (a) The surface structure of Si(100)-2×1, (b) the scheme of buckling Si═Si dimer and (c) the schematic presentation of asymmetric [2+2] cycloaddition for alkene to Si(100)-2×1.

more complicated. It was suggested that benzene can bind to Si(100) through both $[4+2]$-like or/and tight-bridge *tetra*-sigma binding modes.[25] For pyridine on Si(100),[35] dative-bonded pyridine via Si:N and $[4+2]$-like cycloadduct involving both N^1 and C^4 are coexistent at low temperatures. At 350 K, dative-bonded molecules possibly convert to *di-sigma* binding configuration.

As a typical substitution of aromatic hydrocarbons, phenylacetylene is made of phenyl ring and conjugated C≡C group. Investigating its interaction with Si surfaces will provide the correlation of reaction selectivity and binding configuration with the individual functional groups in a multifunctional molecule, offering the necessary flexibility in functionalization and modification of silicon surfaces.

In this experiment, high-resolution electron-energy-loss spectroscopy (HREELS) and x-ray photoelectron spectroscopy (XPS) were employed to characterize the vibrational and electronic properties of phenylacetylene and phenylacetylene-α-d_1 on Si(100)-2×1, respectively. Density Functional Theory (DFT) calculations were commanded to optimize the chemisorption geometries and calculate their adsorption energies. Our results show that phenylacetylene is covalently bound to Si(100)-2×1 through a $[2+2]$-like cycloaddition of the C≡C with a Si=Si dimer, forming a styrene-like conjugation structure. The resulting conjugation structures may be considered as a precursor for further syntheses, modification, and creation of multilayer molecular architectures on silicon surfaces.

II. EXPERIMENT

The experiments were performed in two separate UHV chambers. Both of them have a base pressure of $<2\times10^{-10}$ Torr, achieved with turbomolecular and sputtered-ion pumps. The investigation of vibrational properties was carried out in a HREELS chamber with a high-resolution electron-energy-loss spectrometer (HREELS, LK-2000-14R) and a quadruple mass spectrometer (UTI-100) for gas analysis. HREELS spectra were taken in a specular geometry on both the clean and phenylacetylene adsorbed samples with primary beam energy of 5.0 eV. A resolution of ~50 cm^{-1} [full width at half maximum (FWHM) for the elastic peak] can be routinely achieved. The off-specular spectra were also collected at off-specular directions of $\Delta\theta$, where the $\Delta\theta$ refers to the angle of $\theta_{(analyzer)}-\theta_{(specular)}$.

The second UHV chamber was mainly equipped with an x-ray gun (both Mg and Al anodes) and hemispherical electron energy analyzer (CLAM 2, VG) for XPS. In the studies of C 1s photoemission, the Mg-anode x-ray source ($h\nu=1253.6$ eV) was used. The binging energy (BE) scale of all the spectra presented in this paper is referenced to the peak maximum of the Si 2p line (99.3 eV calibrated for Au $4f_{7/2}$) (Ref. 36) of Si(100)-2×1 with a FWHM lower than 1.3 eV. The C 1s photoemission spectra of physisorbed multilayer and saturated chemisorption monolayer were fitted with VGX900 (VG Scientific, UK). During the fitting, the full width at half maximum (FWHM) of each peak was kept at 1.25 eV which is the typical resolution of C 1s core-level for our XPS system
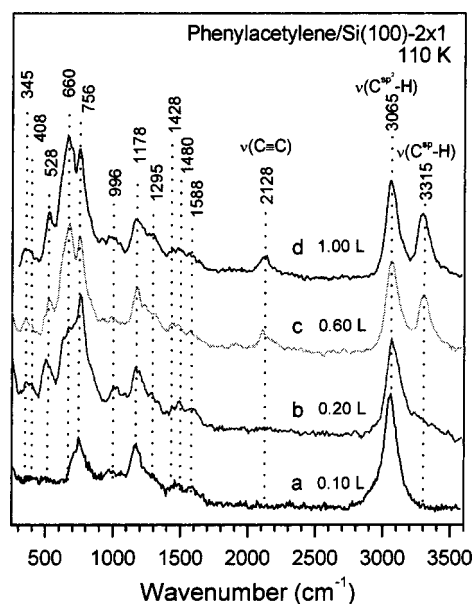

FIG. 2. HREELS spectra of phenylaceetylene-exposed Si(100)-2×1 at 110 K as a function of exposure.

The samples with a dimension of $8\times18\times0.38$ mm^3 were cut from *n*-type Si(100) wafers (*Phosphors* doped, with a resistivity of 1–30 Ω cm, 99.999%, Goodfellow). A Ta-sheet heater (0.025 mm thick, Goodfellow) was sandwiched tightly between two Si(100) crystals held together by two Ta clips. A 0.003-in W-5% Re/W-26% Re thermocouple was attached to the center of the one of the silicon samples using a high-temperature ceramic adhesive (Aremco 516) for temperature measurement and control. Uniform heating of the samples was achieved by passing current through the Ta heater. This sample-mounting configuration allows us to resistively heat the sample to 1400 K and conductively cool them to 110 K using liquid nitrogen. The temperature distribution on the samples is within ±10 K at 1000 K, determined using a pyrometer ($\varepsilon=0.74$, TR-630, Minolta).

The sample was carefully cleaned by cycles of Ar$^+$ sputtering and annealing to 1300 K for 15–20 min. Phenylacetylene (99%, Aldrich) and Phenylacetylene-α-d_1 (99 at. % D, Aldrich) were further purified by several freeze-pump-thaw cycles before being dosed onto the silicon surface through a Varian adjustable leak valve. Exposures were calculated and reported in Langmuir (1 L=10^{-6} Torr s) without ion gauge sensitivity calibration.

III. RESULTS AND DISCUSSION

A. High-resolution electron-energy-loss spectroscopy

Figure 2 shows the high-resolution electron-energy-loss spectra of phenylacetylene-exposed Si(100)-2×1 at 110 K as a function of exposure. The vibrational frequencies and their assignments for physisorbed and chemisorbed molecules are summarized in Table I. Vibrational signatures at 345, 408, 528, 660, 756, 996, 1178, 1295, 1428, 1480, 1588, 2128, 3065, and 3315 cm^{-1} can be clearly identified in the spectrum of physisorbed molecules. Table I shows that the

TABLE I. The assignments of HREELS spectra of physisorbed and saturated chemisorption phenylacetylene on Si(100)-2×1. All frequencies are in cm^{-1}. Phys.: physisorbed molecules; Chem.: Chemisorbed molecules.

Designation	Description	Liquid[a]	Phys.	Chem.	Isotope[a]	Phys.	Chem.
ν_1	$\nu\equiv$C-H(D)	3332	3315		2609	2578	
	$\nu=$C-D						2218
ν_{25}	νC-H	3096			3096		
ν_2	νC-H	3078			3078		
ν_3	νC-H	3067	3065	3060	3066	3067	3052
ν_{26}	νC-H	3058			3058		
ν_4	νC-H	3047			3046		
ν_5	νC$\equiv$C	2120	2128		1984	1984	
	νC$=$C			1630			1618
ν_6	νC-C	1601	1588	1589	1600	1582	1588
ν_{27}	νC-C	1573			1573		
ν_7	νC-C	1488	1480	1484	1488	1485	1480
ν_{28}	νC-C	1447	1428	1426	1447	1429	1425
ν_{29}	νC-C	1330			1329		
ν_{30}	βC-H	1282	1295	1298	1278	1288	1288
ν_8	νC-CCH	1192			1193	1206	
ν_9	βC-H	1175	1178	1168	1175	1165	1160
ν_{31}	βC-H	1157			1157		
ν_{32}	βC-H	1070		1065	1070		
ν_{10}	βC-H	1028			1025		
ν_{11}	ring breath	998	996	988	998		
ν_{17}	γC-H	985			985	1002	
ν_{14}	γC-H	968			968		963
ν_{18}	γC-H	915			916		
ν_{15}	γC-H	842			841		
ν_{12}	αC-C-C	760	756	745	758	758	752
ν_{19}	γC-H	756			758		
ν_{20}	ϕC-C	689	660		691	695	687
ν_{33}	βCC-H(D)	649			482		
ν_{34}	αC-C-C	613			623		
ν_{21}	γCC-H(D)	613			482		
ν_{22}	ϕC-C	530	528		531	523	
ν_{35}	β(C-C$\equiv$C)	513			531		
	νSi-C			510			515
ν_{13}	αC-C-C	465			459		
ν_{16}	ϕC-C	418	408	396	419		
ν_{23}	γC-CCH	349	345		340	350	
ν_{36}	βC-CCH	349			340		
ν_{24}	γC-C$\equiv$C	162			154		

[a]Reference 37.

vibrational features of physisorbed phenylacetylene [Figs. 2(c) and (d)] are in excellent agreement with the IR spectrum of liquid phenyacetylene.[37] Among these vibrational signatures of physisorbed molecules, the peak at 3315 cm^{-1} is assigned to the C^{sp}-H (-C$\equiv$CH) stretching mode; the loss feature at 3065 cm^{-1} is attributable to the stretching mode of C^{sp2}-H on phenyl ring; the C$\equiv$C stretching mode can account for the feature at 2128 cm^{-1}; vibrational features around 1588, 1480, 1428, and 1295 cm^{-1} are associated with the characteristic vibrational modes of monosubstituted phenyl ring.[38,39]

The vibrational features of chemisorbed phenylacetylene at low exposures [Fig. 2(a)] are obtained by annealing the multilayer phenylacetylene-exposed sample to 300 K to drive away all the physisorbed molecules and only retain the chemisorbed molecules [Fig. 3(b)], however, are significantly different. Losses at 396, 510, 745, 988, 1065, 1168, 1298, 1426, 1484, 1589, 1630, and 3060 cm^{-1} can be readily resolved. The absence of observable Si-H stretching around 2000–2100 cm^{-1} (Ref. 40) suggests the nature of molecular chemisorption for phenylacetylene on Si(100)-2×1. Compared to physisorbed molecules, the vibrational peak around
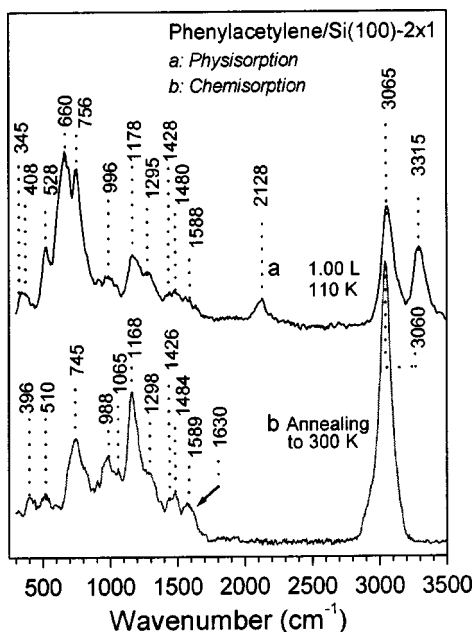
FIG. 3. HREELS spectra of the physisorbed multilayer (a) and saturated chemisorption monolayer (b) of phenylacetylene on Si(100)-2×1.
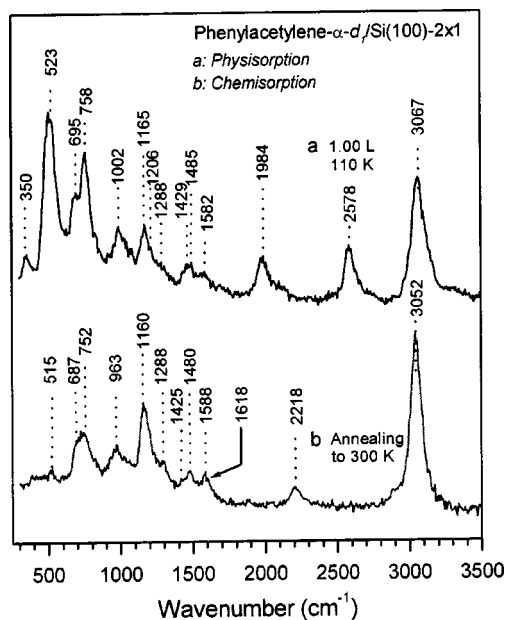

FIG. 4. HREELS spectra of the physisorbed multilayer (a) and saturated chemisorption monolayer (b) of phenylacetylen-α-d_1 on Si(100)-2×1.

3315 cm^{-1} associated to C^{sp}-H (in -C≡CH) stretching mode is absent in chemisorbed molecules, demonstrating the rehybridization of carbon atoms of the C≡C group and their involvement in binding with the Si surface. This is further supported by the absence of C≡C stretching mode around 2128 cm^{-1} in the vibrational signatures of chemisorbed phenylacetylene [Figs. 2(a) and 3(b)]. In addition, a new peak at 1630 cm^{-1} attributed to C=C double bond can be identified although its relative intensity is low possibly due to its nearly parallel orientation.[41] Another change is the appearance of a new peak at ~510 cm^{-1}, ascribed to Si-C stretching mode.[42] Furthermore, the characteristic vibrational modes [ν(C-C)] of monosubstituted phenyl ring around 1580–1650 cm^{-1}, 1450–1525 cm^{-1}, and 1280–1350 cm^{-1} are preserved in the HREELS spectra of chemisorbed phenylacetylene [Fig. 3(b)], indicating the retention of aromaticity of phenyl ring. The fact of no observable intensities around 2900 cm^{-1} suggests that there are no carbon atoms rehybridizing from sp^2 or sp into sp^3 after chemisorption, further supporting the preservation of phenyl ring upon chemisorption.

The absence of C^{sp}-H and C≡C stretching modes in chemisorbed molecules indicates the direct involvement of C≡C group in the reaction with Si=Si dimer. The negligible vibrational feature for C^{sp3}-H stretching mode at <3000 cm^{-1} together with retention of the characteristic vibrational modes [ν(C-C)] of monosubstituted phenyl ring demonstrates that the chemical binding occurs mainly through the external C≡C group. Thus the [2+2]-like cycloaddition between C≡C group and Si dimer is the proposed binding mode.

For further understanding the reaction mechanism and clarifying binding structure for phenylacetylene on Si(100)-2×1, phenylacetylene-α-d_1 was also employed in our HREELS experiments. Figures 4(a) and (b) present the

vibrational features of physisorbed and saturated chemisorption phenylacetylene-α-d_1 on Si(100)-2×1, respectively. In Fig. 4(a), vibrational peaks at 350, 523, 695, 758, 1002, 1165, 1206, 1288, 1429, 1485, 1582, 1984, 2578, and 3067 are clearly resolved. Their assignments listed in Table I show that the vibrational features of physisorbed molecules are in good accordance with the IR spectrum of liquid phenylacetylene-α-d_1.[37] Among these vibrational signatures, the two peaks at 2578 and 1984 cm^{-1} are assigned to C$^{\alpha(sp)}$-D (-C≡CD) and C≡C stretching modes, respectively. The feature at 3067 cm^{-1} is ascribed to the C^{sp2}-H stretching of phenyl ring. For chemisorbed molecules, both C$^{\alpha(sp)}$-D and C$^{\alpha}$≡C$^{\beta}$ stretching modes at ~2578 and ~1984 cm^{-1}, respectively, are absent. However, a new peak appears around 2218 cm^{-1}, attributable to the C^{sp2}-D stretching mode.[43] Indeed, these changes occurred at C-D and C-H stretching regions upon chemisorption of phenylacetylene-α-d_1 strongly support the conclusion that only C≡C bond directly participates in the covalent binding with the silicon surface.

Figure 5 presents seven possible binding modes of phenylacetylene on Si(100)-2×1. Among them, modes I, II, III, IV, and V are the cycloadducts between phenyl ring and Si surface dangling bonds by [2+2]-like or [4+2]-like reaction schemes. Their C-H stretching features would present two separate peaks corresponding to C^{sp3}-H and C^{sp2}-H together with C^{sp}-D stretching remaining at the similar frequency (at ~2578 cm^{-1}) to that of physisorbed phenylacetylene-α-d_1. However, our experimental results (Fig. 4) exclude the occurrence of these possibilities. In mode VI, both external -C≡CH and its conjugated internal C=C of phenyl ring take part in the covalent attachment with the Si=Si dimer through [4+2]-like addition strategy. In the resulting configuration, the C$^{\alpha}$ rehybridizes from sp to
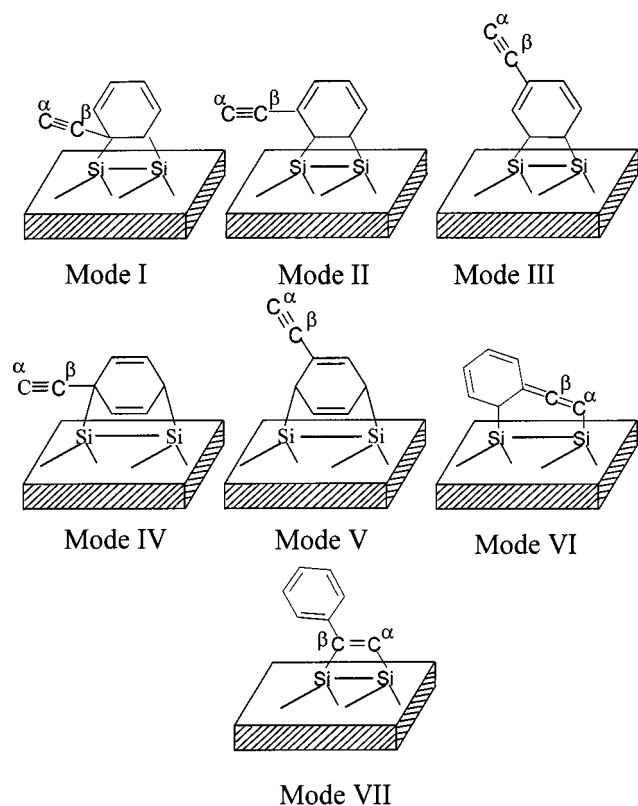
FIG. 5. The schematic diagram of seven possible binding modes of phenylacetylene covalently bound to Si(100)-2×1.
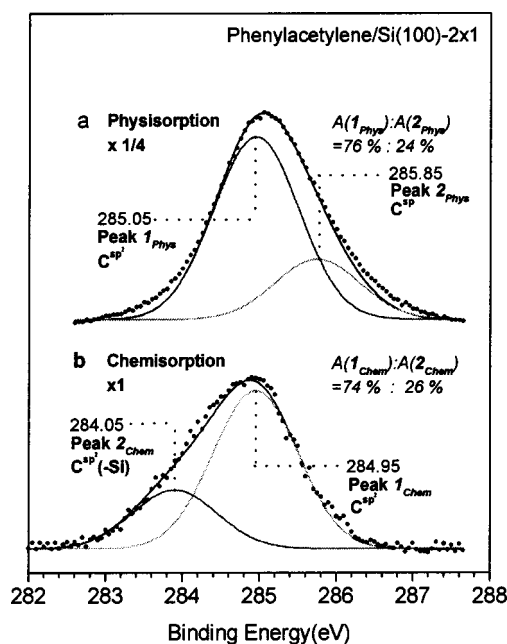

FIG. 6. C $1s$ experimental spectra and their deconvoluted results of physisorbed multilayer (a) and saturated chemisorption monolayer (b) on Si(100)-2×1.

sp^2 and one carbon atom of phenyl ring changes from sp^2 to sp^3. Thus the disappearance of both C^{sp}-H stretching feature and the characteristic vibrational peaks of monosubstituted phenyl ring would be expected in chemisorbed molecules. The C^{sp3}-H stretching at <3000 cm^{-1} would be concurrently observed with the C^{sp2}-H stretching around 3050 cm^{-1}. In fact, our major experimental evidences of (i) the disappearance of both C^{sp}-H and C≡C stretching modes, (ii) only C-H stretching mode around 3050 cm^{-1} (C^{sp2}-H stretching), and (iii) the preservation of characteristic vibrational modes of monosubstituted phenyl ring, eliminate the possibility of mode VI. In addition, due to the absence of C^{sp3}-H(D) stretching mode in Figs. 3(b) and 4(b), a *tetra-σ* binding mode, similar to acetylene on Si(100)-2×1, can be ruled out.[44–47] Our experimental spectra can be well interpreted with the proposed mode VII, the [2+2]-like cycloaddition pathway involving the C≡C group and one Si=Si dimer. In this binding mode, due to the rehybridization of C^α and C^β atoms from sp to sp^2, all the carbon atoms in the chemisorbed molecules have a sp^2 configuration, resulting in a single C-H stretching peak around 3060 cm^{-1} in the spectra of chemisorbed phenylacetylene. The C^α-D stretching in phenylacetylene-α-d_1 will significantly down-shifts from 2578 cm^{-1} ascribed to C^{sp}-D for physisorbed molecules to 2218 cm^{-1} attributed to the C^{sp2}-D stretching mode[43] due to the direct involvement of C≡C in the surface reaction. This binding configuration is further supported by the absence of C≡C stretching modes at 1984 cm^{-1} [Fig. 4(b)]. Moreover, the retention of characteristic vibrational features of mono-

substituted phenyl ring upon chemisorption shows that phenyl ring does not directly interact with the Si surface. Based on these experimental evidences, it is reasonable to propose that phenylacetylene covalently binds to Si(100)-2×1 through [2+2]-like cycloaddition between the C≡C group and Si=Si dimer.

B. X-ray photoelectron spectroscopy

XPS was employed to investigate the chemical shifts of C $1s$ core level of phenylacetylene on Si(100)-2×1. C $1s$ photoemission feature for physisorbed multilayer on Si(100)-2×1 is presented in Fig. 6(a). Figure 6(b) is the C $1s$ spectra for saturated chemisorption monolayer on Si(100)-2×1 obtained by annealing the multilayer phenylacetylene covered sample to 300 K to drive away physisorbed phenylacetylene and only remain chemisorbed molecules. For both systems, the experimental C $1s$ spectra display an asymmetric peak shape, possibly due to the existence of inequivalent carbon atoms. In order to assign C $1s$ peaks of physisorbed and chemisorbed phenylacetylene, software VGX900 (VG) (Ref. 48) was commanded to deconvolute the XPS spectra. The fitting results presented in Fig. 6 show that the C $1s$ peak for physisorbed phenylacetylene can be reasonably deconvoluted into two peaks at 285.85 and 285.05 eV with an area ratio of ~1:3, assigned to the C≡C group and phenyl ring, respectively. Similarly, C $1s$ photoemission feature of chemisorbed molecules can be fitted into two peaks at 284.95 and 284.05 eV with an intensity ratio of ~3:1. According to the HREELS results, chemisorbed phenylscetylene has a styrene-like skeleton. In this structure, six C atoms of phenyl ring maintain their sp^2 hybridization upon chemisorption; the other two C atoms with the hybridization of sp^2 are covalently linked to surface sili-

TABLE II. Adsorption energies of the local minima in the phenylacetylene/Si_9H_{12} model system from B3LYP/6-311+G(d). All energies are in kcal mol^{-1}.

Reactive functionality	Phenyl ring	Phenyl ring	Phenyl ring	Phenyl ring	Phenyl ring	-C≡C-C≡C-	C≡C
Binging mode in Fig. 5	I	II	III	IV	V	VI	VII
Reaction mechanism	[2+2]-like	[2+2]-like	[2+2]-like	[4+2]-like	[4+2]-like	[4+2]-like	[2+2]-like
Adsorption energy	−0.4	5.3	3.8	15.8	20.9	27.0	54.9

Adsorption energy is calculated by subtracting the energy of cluster (C_8H_6/Si_9H_{12}) from the total energy of free substrate cluster (Si_9H_{12}) and gas phase phenylacetylene (C_8H_6).

con atoms. Thus the peaks at 284.95 and 284.05 can be reasonably assigned to the C atoms of phenyl ring and those of external group [-(Si)C$^\alpha$=C$^\beta$(Si)H], respectively. Compared to physisorbed molecules, the C 1s core level of phenyl ring does not display obvious chemical shift, which also suggests that phenyl ring is not directly involved in the binding with Si surfaces. However, the binding energy of C$^\alpha$ and C$^\beta$ significantly shifts down by 1.8 eV due to their rehybridization from sp to sp^2 and covalent binding to Si atoms with a lower electronegativity. Thus our XPS results are consistent with vibrational analyses and further confirm the direct participation of C≡C in the cycloaddition with Si=Si dimers.

C. DFT calculations

In general, there are seven possible binding modes for phenylacetylene chemically binding on Si(100), schematically presented in Fig. 5. The direct interaction between phenyl ring and Si dimer is presented in modes I–V. In addition, there are other two possibilities including the [4+2]-like cyclic addition involving both the external C≡C group and its conjugated C=C on phenyl ring (mode VI) and the direct participation of the external C≡C group via a [2+2]-like cycloaddition pathway (mode VII). Our DFT studies focus on the geometric optimization and adsorption energy calculation for further understanding our experimental results.

We performed DFT calculations using GAUSSIAN 94 (Ref. 49) for a phenylacetylene molecule adsorbed onto a starting cluster of Si_9H_{12}. This cluster with one exposed Si=Si dimer was successfully used in several previous studies.[50–53] Based on the possible binding modes shown in Fig. 5, seven phenylacetylene-bonded calculation clusters (not shown) were built to model their corresponding cycloadducts. All

DFT studies are single point energy calculation of B3LYP/6-311+G(d) on the fully optimized geometry of B3LYP/6-31G(d). The calculated adsorption energies of binding modes I–VII are listed in Table II. It is unambiguous that the product of [2+2]-like cycloaddition reaction occurring between the external C≡C group and Si=Si dimer (mode VII) has the largest adsorption energy. Its value is also much higher than that of [4+2]-like cycloadduct (mode VI) involving both C≡C and its conjugated C=C bond on phenyl ring. The calculation result clearly shows that the energetically preferred reaction mechanism for phenylacetylene is distinctly different from the [4+2]-like cycloaddition for typical conjugated dienes on Si(100)-2×1, such as 1,3-cyclohexadiene[21–23] and 1,3-butadiene.[24] However, this preferable [2+2] cycloaddition mechanism for phenylacetylene is similar to benzonitrile on Si(100)-2×1 via the [2+2]-like approach occurring at C≡N group to form a benzoimine-like conjugation skeleton.[34] In both cases, the cycloaddition results in an energetically stable aromatic skeleton on surfaces.

IV. SUMMARY

Our experimental results together with DFT calculations have shown the formation of styrene-like conjugation structures for phenylacetylene on Si(100)-2×1 through the [2+2]-like addition reaction scheme between the external C≡C group and Si=Si dimer. The formed styrene-like skeleton may possibly be employed as a precursor for further chemical modification and functionalization of silicon surfaces, an intermediate for organic syntheses in vacuum, or as a monomer for fabrication of conductive polymer thin films on semiconductors.[11–12,54]

*Corresponding author. Fax: (65) 6779 1691; email address: chmxugq@nus.edu.sg

[1] J. T. Yates, Jr., Science **279**, 335 (1998).

[2] R. A. Wolkow, Annu. Rev. Phys. Chem. **50**, 413 (1999).

[3] J. M. Buriak, Chem. Commun. (Cambridge) **12**, 1051 (1999).

[4] H. N. Waltenburg and J. T. Yates, Jr., Chem. Rev. **95**, 1589 (1995).

[5] J. G. Ekerdt, Y. M. Sun, A. Szabo, G. J. Szulczewski, and J. M. White, Chem. Rev. **96**, 1499 (1996).

[6] L. C. Chen, K. H. Chen, J. J. Wu, D. M. Bhusari, and M. C. Lin, *Silicon-Based Materials and Devices: Materials and Processing*, edited by H. S. Nalwa (Academic, New York, 2001), Vol. 1.

[7] Y. Cui and C. M. Lieber, Science **291**, 851 (2001).

[8] T. H. Lee, Sci. Am. (Int. Ed.) **286**, 52 (2002).

[9] H. G. Craighead, Science **290**, 1532 (2000).

[10] Y. Cui, Q. Wei, H. Park, and C. M. Lieber, Science **293**, 1289 (2001).

[11] T. A. Skotheim, *Handbook of Conducting Polymers* (Marcel Dekker, New York, 1986).

[12] H. S. Nalwa, *Handbook of Organic Conductive Molecules and Polymers* (John Wiley & Sons, New York, 1997).

[13] K. Takayanagi, Y. Tanishiro, and M. Takahashi, Surf. Sci. **164**, 367 (1985); K. Takayanagi, T. Tanishiro, S. Tanahashi, and M. J. Takahashi, J. Vac. Sci. Technol. A **3**, 1502 (1985).

[14] H. B. Liu and R. J. Hamers, J. Am. Chem. Soc. **119**, 7593 (1997).

[15] S. F. Bent, Surf. Sci. **500**, 879 (2002).

[16] R. J. Hamers, S. K. Coulter, M. D. Ellison, J. S. Hovis, D. F. Padowitz, M. P. Schwartz, C. M. Greenlief, and J. N. Russell, Acc. Chem. Res. **33**, 617 (2000).

[17] M. H. Qiao, F. Tao, Y. Cao, Q. Liu, Z. H. Li, W. L. Dai, J. F. Deng, and G. Q. Xu, J. Chem. Phys. **114**, 2766 (2001).

[18] M. H. Qiao, Y. Cao, F. Tao, J. F. Deng, and G. Q. Xu, J. Phys. Chem. B **104**, 11 211 (2000).

[19] M. H. Qiao, Y. Cao, J. F. Deng, and G. Q. Xu, Chem. Phys. Lett. **325**, 508 (2000).

[20] F. Tao, W. S. Sim, G. Q. Xu, and M. H. Qiao, J. Am. Chem. Soc. **123**, 9397 (2001).

[21] R. Konency and D. J. Doren, Surf. Sci. **417**, 169 (1998).

[22] J. S. Hovis, H. B. Liu, and R. J. Hamers, J. Phys. Chem. B **102**, 6873 (1998).

[23] J. S. Hovis, H. B. Liu, and R. J. Hamers, Surf. Sci. **404**, 1 (1998).

[24] A. V. Teplyakov, M. J. Kong, and S. F. Bent, J. Chem. Phys. **108**, 4599 (1998).

[25] Y. Tahuchi, M. Fujisawa, T. Takaoka, T. Okada, and M. Nishijima, J. Chem. Phys. **95**, 6870 (1991).

[26] B. I. Craig, Surf. Sci. **280**, L279 (1993).

[27] G. P. Lopinski, D. J. Moffatt, and R. A. Wolkow, Chem. Phys. Lett. **282**, 305 (1998).

[28] B. Borovsky, M. Krueger, and E. Ganz, Phys. Rev. B **57**, R4269 (1998).

[29] S. Gokhole, P. Trischberger, D. Menzel, W. Widdra, H. Droge, H. P. Steinruck, U. Brikenheuer, U. Gutdeutsch, and N. Rosch, J. Chem. Phys. **108**, 5554 (1998).

[30] P. L. Silverstrelli, F. Ancilotto, and F. Toiogo, Phys. Rev. B **62**, 1596 (2000).

[31] M. Staufer, U. Birkenheuer, T. Belling, F. Nortemann, N. Rosch, W. Widdra, K. I. Kostov, T. Moritz, and D. Menzel, J. Chem. Phys. **112**, 2498 (2000).

[32] M. D. Ellison and R. J. Hamers, J. Phys. Chem. B **103**, 6243 (1999).

[33] S. K. Coulter, J. S. Hovis, M. D. Ellison, and R. J. Hamers, J. Vac. Sci. Technol. A **18**, 1965 (2000).

[34] F. Tao, Z. H. Wang, and G. Q. Xu, J. Phys. Chem. B **106**, 3557 (2002).

[35] F. Tao, M. H. Qiao, Z. H. Wang, and G. Q. Xu (unpublished).

[36] J. F. Moulder, W. F. Stickle, and K. D. Bomben, *Handbook of X-ray Photoelectron Spectroscopy* (Perkin-Elmer Corporation, Minnesota, 1992).

[37] G. W. King and S. P. So, J. Mol. Spectrosc. **36**, 468 (1970).

[38] L. V. Daimay, B. C. Norman, G. F. William, and G. G. Jeanette, *The Handbook of Infrared and Raman Characteristic Frequencies of Organic Molecules* (Academic, Boston, 1991).

[39] G. Varsanyi and S. Szoke, *Vibrational Spectra of Benzene Derivates* (Academic, New York & London, 1969).

[40] H. Wagner, R. Butz, and U. Backes, D. Bruchmann, Solid State Commun. **38**, 1155 (1981).

[41] H. Ibach, D. L. Mills, *Electron Energy Loss Spectroscopy and Surface Vibrations* (Academic, New York, 1982).

[42] K. Hamaguchi, S. Machida, M. Nagao, F. Yasui, K. Mukai, Y. Yamashita, and J. Yoshinobu, J. Phys. Chem. B **105**, 3718 (2001).

[43] D. A. Condirston and J. D. Laposa, J. Mol. Spectrosc. **42**, 466 (1976).

[44] R. Miotto, A. C. Ferraz, and G. P. Srivastava, Phys. Rev. B **65**, 075401 (2002).

[45] W. Kim, H. Kim, G. Lee, Y. K. Hong, K. Lee, C. Hwang, D. H. Kim, and J. Y. Koo, Phys. Rev. B **64**, 193313 (2001).

[46] X. Lu and M. C. Lin, Phys. Chem. Chem. Phys. **2**, 4213 (2000).

[47] S. H. Xu, Y. Yang, M. Keeffe, G. J. Lapeyre, and E. Rotenberg, Phys. Rev. B **60**, 11 586 (1999).

[48] VG Microtech Ltd., VGX900-Real and Protected Mode Programs, UK, 1994.

[49] M. J. Frisch, G. W. Trucks, H. B. Schlegel, P. M. W. Gill, B. G. Johnson, M. A. Robb, J. R. Cheeseman, T. Keith, G. A. Petersson, J. A. Montgomery, K. Raghavachari, M. A. Al-Laham, V. G. Zakrzewski, J. V. Ortiz, J. B. Foresman, J. Cioslowski, B. B. Stefanov, A. Nanayakkara, M. Challacombe, C. Y. Peng, P. Y. Ayala, W. Chen, M. W. Wong, J. L. Andres, E. S. Replogle, R. Gomperts, R. L. Martin, D. J. Fox, J. S. Binkley, D. J. Defrees, J. Baker, J. P. Stewart, M. Head-Gordon, C. Gonzalez, and J. A. Pople, GAUSSIAN 94, Rev. C. W (Gaussian, Inc. Pittsburgh, PA, 1995).

[50] T. Kato, S. Y. Kang, X. Xu, and T. Yamabe, J. Phys. Chem. B **105**, 10 340 (2001).

[51] X. Xu, S. Y. Kang, and T. Yamabe, Bull. Chem. Soc. Jpn. **74**, 817 (2001).

[52] P. L. Silvestrelli, F. Ancilotto, and F. Toigo, Phys. Rev. B **62**, 1596 (2000).

[53] H. A. Hofer, A. J. Fisher, G. P. Lopinski, and R. A. Wolkow, Phys. Rev. B **63**, 085314 (2001).

[54] I. Capek, J. Hernandez-Barajas, D. Hunkelev, J. L. Reddinger, J. R. Reynolds, and C. Wandrey, *Radical Polymerisation Polyelectrolytes* (Springer, New York & Berlin, 1999).